Published in final edited form as:
Int J Cancer. 2011 August 1; 129(3): 553–564. doi:10.1002/ijc.25954.

Overexpression of the dynein light chain km23-1 in human ovarian carcinoma cells inhibits tumor formation *in vivo* and causes mitotic delay at prometaphase/metaphase

Nageswara R. Pulipati, **Qunyan Jin**, **Xin Liu**, **Baodong Sun**, **Manoj K. Pandey**, **Jonathan P. Huber**, **Wei Ding**, and **Kathleen M. Mulder**[1]
Department of Biochemistry and Molecular Biology, Penn State Hershey College of Medicine, Hershey, PA 17033

Abstract

km23-1 is a dynein light chain that was identified as a TGFß receptor-interacting protein. To investigate whether km23-1 controls human ovarian carcinoma cell (HOCC) growth, we established a tet-off inducible expression system in SKOV-3 cells in which the expression of km23-1 is induced upon doxycycline removal. We found that forced expression of km23-1 inhibited both anchorage-dependent and anchorage-independent growth of SKOV-3 cells. More importantly, induction of km23-1 expression substantially reduced the tumorigenicity of SKOV-3 cells in a xenograft model *in vivo*. Fluorescence-activated cell sorting analysis of SKOV-3 and IGROV-1 HOCCs demonstrated that the cells were accumulating at G2/M. Phospho-MEK, phospho-ERK, and cyclin B1 were elevated, as was the mitotic index, suggesting that km23-1 suppresses HOCCs growth by inducing a mitotic delay. Immunofluorescence analyses demonstrated that the cells were accumulating at prometaphase/metaphase with increases in multipolar and multinucleated cells. Further, while the mitotic spindle assembly checkpoint protein BubR1 was present at the prometaphase kinetochore in Dox+/− cells, it was inappropriately retained at the metaphase kinetochore in Dox− cells. Thus, the mechanism by which high levels of km23-1 suppresses ovarian carcinoma growth *in vitro* and inhibits ovary tumor formation *in vivo* appears to involve a BubR1-related mitotic delay.

Keywords

dynein; km23-1; ovarian cancer; mitosis

Introduction

Epithelial ovarian cancer is one of the most common forms of ovarian cancer and the most lethal gynecologic malignancy among women in the United States, with 21,880 new cases and 13,850 deaths estimated in 2010.[1] While microtubule (MT)-binding agents, such as paclitaxel (taxol), are being used in the treatment of ovarian cancer, acquired and intrinsic drug resistance has significantly limited their efficacy. Thus, it is critical to develop novel, targeted therapeutics for ovarian cancer. More recently, the motors that move along the spindle MTs have been targeted for the development of new therapies. For example, the kinetochore-associated mitotic motor kinesin, termed centromere-associated protein-E (CENP-E), has been targeted due to its key role in the mitotic spindle assembly checkpoint

[1]To whom correspondence should be addressed: Department of Biochemistry and Molecular Biology-MC H171, Penn State Hershey College of Medicine, 500 University Drive, Hershey, PA 17033, Telephone: 717-531-6789; FAX: 717-531-0939, kmm15@psu.edu.

(SAC).[2] Thus, motor protein regulatory agents may offer promise for providing improved efficacies with reduced side effects in the treatment of ovarian cancer and other human malignancies.[3]

While the plus-end-directed kinesin MT motor has been targeted for the development of anti-cancer therapeutics, the minus-end-directed motor protein dynein has not received similar attention in terms of its targeting potential. Although dynein's important functions in inactivating the SAC have been widely studied,[4, 5] little is known about how regulation of dynein functions can contribute to ovarian cancer development or progression. We have identified a novel TGFß receptor-interacting protein, termed km23-1,[6] which is also a light chain of the motor protein dynein (also called DYNLRB1/LC7-1/robl-1/DNLC2A/DYRB1).[7-11] Further, we have reported that km23-1 plays a critical role in normal TGFß signaling.[6, 10, 12-14] However, many ovarian carcinoma cells are resistant to the growth inhibitory effects of TGFß.[15, 16] Accordingly, in order to define the role of the km23-1 dynein light chain (DLC) in ovarian carcinogenesis, we investigated whether forced expression of wild-type km23-1 could regulate cell growth and tumor progression of TGFß-resistant HOCCs.

Here we demonstrate that overexpression of km23-1 in the highly aggressive SKOV-3 HOCCs inhibited both monolayer proliferation and anchorage-independent growth of the cells, causing an accumulation of cells in mitosis at prometaphase/metaphase. Further, BubR1 was aberrantly retained at the kinetochore in metaphase cells with high levels of km23-1, suggesting that the SAC had remained active. More importantly, induction of km23-1 expression reduced the tumorigenicity of the HOCCs in a xenograft model. Thus, overexpression of the DLC km23-1 can function to decrease HOCC growth *in vitro* and tumor formation *in vivo* through a BubR1-related role in metaphase cells.

Materials and Methods

Reagents

The antibodies used were: polyclonal anti-Flag (F7425, Sigma-Aldrich, St. Louis, MO), anti-glyceraldehyde-3-phosphate dehydrogenase (GAPDH) (ab8245, Abcam, Cambridge, MA), anti-dynein intermediate chain (DIC) (MAB 1685, Chemicon, Temecula, CA), human CREST (Immunovision, Springdale, AR), Mouse BubR1 (BD Bioscience, San Jose, CA), or mouse BubR1 (Millipore, Billerica, MA) and antibodies against cyclin B1 (4138S), phospho-histone H3 (9706S), phospho-MEK1/2 (9121S), MEK1/2 (9122), phospho-ERK1/2 (4370S), and ERK1/2 (4780) were from Cell Signaling Technology (Denvers, MA). Annexin V-Fluos staining kit was from Roche Applied Science (Indianapolis, IN). Other chemicals were obtained from Sigma unless otherwise indicated.

Cell Culture

SKOV-3 cells were purchased from American Type Culture Collection (Manassas, VA) and cultured as described thereby. The IGROV-1 cell line was a gift from D. MacLaughlin (Massachusetts General Hospital, Boston, MA). OVCA433 cells were obtained from R. Bast (M.D. Anderson Cancer Center, Houston, TX). IGROV-1 and OVCA433 cells were cultured as described.[12] Cells were routinely screened for *mycoplasma* using Hoechst 33258 staining.

DNA Constructs

Flag-tagged km23-1 constructs were generated by inserting the corresponding PCR products into pFlag-CMV5a[6] or pBIG2r.[17]

Generation of km23-1 Tet-off Expression System in SKOV-3 Cells

To generate inducible cells that over-express wild-type km23-1, SKOV-3 cells were transfected with the pBIG2r empty vector (EV) or pBIG2r-km23-1-Flag using Fugene 6 according to the manufacturer's instructions. After transfection, cells were selected with hygromycin B (400 μg/ml) and either pooled or cloned by limiting dilution. Clones and pools were screened for km23-1-Flag expression after Dox removal by immunoblotting and were maintained in medium containing hygromycin B (400μg/ml) and Dox (2μg/ml). **Immunoblot Analyses** were performed as described.[6, 10, 18]

Cell Proliferation Assays

SKOV-3-pBIG2r EV pool (EV pool), km23-1 pool, and km23-1 clones cells were plated at 6.3×10^3 cells/cm^2, treated +/−Dox, and were analyzed using a crystal violet assay.[6] Routine cell growth assays were also performed using the Vi-CELL Series Cell Viability Analyzer (Beckman Coulter, Brea, CA).

Soft Agar Growth Assays were performed as described[19] except that 5.2×10^3/cm^2 cells were plated in 0.3% agar on top of the 0.8% agar bottom layer +/−Dox. Colonies were scored by microscopy after 21d.

FACS Analysis was used to determine cell cycle distribution as described.[12] **Immunofluorescence analyses** were performed in cells grown in chamber slides +/− Dox for 9-14d when mitotic delay was detectable in Flag-positive cells. **For Mitotic Index**, cells were fixed, permeabilized,[10] and incubated with mouse monoclonal anti-α-tubulin (1:1200), mouse monoclonal anti-phospho-histone H3 (1:1200), or rabbit polyclonal anti-Flag (1:600). Phospho-histone H3-positive cells, Flag-positive cells, and total cell numbers were determined for each experiment from between 500-1000 of each of +/−Dox cells. **For kinetochore studies**, immunofluorescence analyses were performed as described.[20] Primary antibodies used were mouse BubR1 (1:100), human CREST (1:1000), and rabbit polyclonal anti-Flag (1:500). For secondary fluorescence staining, cy3-conjugated goat anti-rabbit IgG (1:400, Jackson ImmunoResearch Laboratories), Alexa 568 goat anti-mouse IgG (1:500), Alexa 488 goat anti-mouse IgG, Alexa 488 goat anti-rabbit IgG, or Alexa 488 goat anti-human IgG (1:200, Invitrogen) were used. Nuclear DNA was stained with 4,6-diamidino-2-phenylindole (DAPI). Images were captured on the same day using identical parameters on an Olympus I×81 microscope coupled with MetaMorph software.

Quantification of multipolar spindles and multinucleated cells

For multipolar cells, a minimum of 20 fields and a total 100 cells were counted for each of three independent experiments as described previously.[21] For multinucleated cells, an average of 450 cells from a minimum of 25 fields were counted, and the percentages of multinucleated cells (>2N and >4N) were scored as described[22] in a cumulative fashion during the period when the Flag-positive cells were undergoing mitotic delay.

Annexin V assay

km23-1 clone #14 cells were grown in 35 mm dishes +/−Dox for 9-14d, and the Annexin V-Fluos kit was used as described by the manufacturer. FACS analyses were performed every other day, values for early (annexin-positive only) and late (annexin- and PI-positive) apoptotic cells were combined, and cumulative apoptotic populations were normalized by number of days.

In vivo Tumorigenicity Studies

Athymic female Balb/c nude mice were obtained from Charles River Laboratories (Wilmington, MA, USA). EV pool, km23-1 pool, and km23-1 clone #14 cells (3.5×10^6) were inoculated subcutaneously into the right flank of mice (eight mice per group), fed continuously with Dox+ chow (20mg/kg) (Bio-Serv, Frenchtown, NJ) or regular chow (Dox −). Tumorigenicities were determined as described.[23, 24]

Statistical analyses

Student's *t* tests were performed with Prism 4 software.

Results

Generation of a km23-1 Tet-off-inducible expression system in SKOV-3 cells

In order to explore novel functions of km23-1 in TGFß-resistant HOCCs, we established a km23-1 tet-off-inducible expression system in the highly aggressive and TGFß-resistant SKOV-3 HOCCs. Western blot analyses in Fig. 1A demonstrate induction of km23-1-Flag expression in km23-1 pool cells, and in two of the representative clones (#14, #12) upon Dox removal. In contrast, EV pool cells did not express km23-1-Flag in +/−Dox. We also calculated the levels of induction of km23-1-Flag expression over endogenous levels. Quantitation of densitometric scans of Western blot analyses revealed that relative levels of km23-1-Flag expression after growth in -Dox for 6-14d were approx. 9-17-fold higher than endogenous km23-1 protein expression levels (data not shown). Thus, the high levels of km23-1 induced in this model were used to perturb the normal functions of the km23-1 DLC, and do not reflect physiological levels of km23-1.

km23-1 inhibits the monolayer cell proliferation and anchorage-independent growth of SKOV-3 cells

To test whether induction of km23-1 expression in SKOV-3 cells causes growth inhibition, EV pool, km23-1 pool, and clone #14 cells were cultured in +/−Dox, and cell growth was monitored daily by crystal violet assays. The results in Fig. 1B (top panel) demonstrated that the proliferation of SKOV-3 EV pool cells was not changed in +/−Dox. However, in km23-1 pool and km23-1 clone #14 cells, cell growth was significantly decreased upon Dox removal (middle and bottom panels). This growth inhibitory effect was also observed in clones 10 and 12 (data not shown).

To further examine whether km23-1 overexpression would affect the malignant potential of SKOV-3 cells, we examined the anchorage-independent growth of EV pool, km23-1 pool, and km23-1clone #14 cells in soft agar growth assays. As shown in Fig. 1C, the number of colonies formed in soft agar was significantly reduced in km23-1 clone #14 and pool Dox− cells in comparison to Dox+ cells. Therefore, forced expression of km23-1 in SKOV-3 cells inhibited both anchorage-dependent and -independent growth of the cells.

Induction of km23-1 expression results in G2/M delay in HOCCs

To address the mechanism by which km23-1 inhibited SKOV-3 cell growth, we performed FACS analyses on EV pool and km23-1 clone #14 cells cultured in +/−Dox. No significant change in the cell cycle distribution was found in the EV pool cells following Dox removal (Fig. 2A, boxed panel, top), whereas the km23-1 clone #14 cells exhibited an increase in the percentage of cells in G2/M from 8.4% to 21.3% at 12d after Dox removal (Fig. 2A, boxed panel, middle). Similarly, Dox removal in km23-1 pool cells resulted in a 1.7-fold increase in the percentage of cells in G2/M (data not shown). FACS analyses of two additional km23-1 clones, clone #10 (Fig. 2A, boxed panel, bottom) and clone #12 (data not shown, ~

2-fold increase), further confirmed the effect of Dox removal on the percentage of cells in G2/M. The level of km23-1-Flag induction upon Dox removal in clones #10 and #14 is shown in the Western blot analyses (Fig. 2A, lower panel).

In order to assess the generality of our findings, two other TGFβ-resistant HOCCs, IGROV-1 and OVCA433, were transiently transfected with km23-1-Flag and cell cycle analysis was performed. As shown in Fig. 2B, wild-type km23-1-Flag expression was highly induced and this induction of km23-1-Flag expression resulted in a 2.5-fold increase in the percentage of cells in G2/M in IGROV-1 cells (Fig. 2B, top and bottom panels). Similarly, when km23-1-Flag expression was highly induced in OVCA433 cells, a 2-fold increase in the percentage of cells in G2/M was observed (data not shown), confirming the results observed for SKOV-3 cells.

Further analyses of the mitotic index in SKOV-3 Dox+/− cells, using the mitotic-specific marker phospho-histone H3, demonstrated that overexpression of km23-1 in clone #14 +Dox cells significantly increased the number of mitotic cells (Fig. 2C, photos). The percentage of cells in mitosis was increased by 9-fold when comparing the +/−Dox cells, the difference being statistically significant with a value of $p < 0.05$ (Fig. 2C, bottom). Together, these results demonstrate that km23-1 exerts its growth regulatory function in TGFß-resistant HOCCs by delaying cells in mitosis. Thereafter, experiments were performed after 7d −Dox, when the Flag-positive cells began displaying a mitotic delay.

Induction of km23-1 expression in HOCCs results in mitotic accumulation of cells prior to the anaphase transition in prometaphase/metaphase

Since we have shown that km23-1 overexpression causes a mitotic delay in the HOCCs, it was of interest to determine at which phase of mitosis the cells were accumulating. Therefore, we examined markers (such as cyclin B1, phospho-ERK and phospho-MEK) known to be increased in mitosis, but which are degraded or reduced in their activity before the anaphase transition can proceed.[25-27] As shown in Fig. 3A, cyclin B1, phospho-MEK, and phospho-ERK remained significantly elevated in SKOV-3 cells upon km23-1 induction, indicating that anaphase onset had not yet occurred in these cells.

Further, to more accurately assess the percentage of cells in the various phases of mitosis in +/−Dox, we performed immunofluorescence analyses of MT's using α-tubulin staining. As depicted in Fig. 3B, the majority of cells with over-expressed km23-1-Flag (−Dox) were in prometaphase/metaphase (65-75%). Altogether, the data suggest that km23-1 overexpression causes cells to accumulate at prometaphase/metaphase.

Overexpression of km23-1 results in aberrant metaphase cells with altered BubR1 localization and the formation of multipolar spindles and multinucleated cells

Thus far, our results have shown that forced expression of km23-1 in HOCCs causes a delay in mitosis at prometaphase/metaphase. Since there is a critical mammalian checkpoint at this point in the cell cycle,[28, 29] it was of interest to determine whether regulation of this SAC would be altered in the −Dox SKOV-3 HOCCs. Accordingly, we analyzed the subcellular distribution of the SAC protein BubR1 by immunofluorescence microscopy in clone #14 +/−Dox cells. As shown in Fig. 4A, in these −Dox cells at prometaphase, both BubR1 and km23-1 were co-localized at kinetochores (1st row). The white staining in the merge shows that some km23-1-Flag and BubR1 are co-localized at the kinetochore at this point. The CREST antiserum stains the inner kinetochore, and the merge (white) demonstrates that some km23-1 is also co-localized with CREST at the kinetochore (2nd row). The kinetochore localization of BubR1 was also confirmed by co-staining of BubR1 and CREST (3rd row). In contrast, in metaphase cells, multiple spots of BubR1 were detected abnormally

localized in both kinetochores and cytoplasm, whereas km23-1 was localized along spindle fibers with little BubR1 co-localization (1st row). As expected, km23-1 was detected at the kinetochore (2nd row), as well as along the spindle fibers (1st row), indicating that km23-1 is involved in the transport of cargos such as SAC proteins from the kinetochore to the spindle pole. The aberrant localization of BubR1 was apparent from the photos showing co-staining of BubR1 with CREST (3rd row). The chromatin organization at the metaphase plate was also altered, as depicted by the DAPI staining (blue).

The situation in Dox+ cells, with only endogenous levels of km23-1, is quite different. As shown in Fig. 4B, in prometaphase, BubR1 was still localized at kinetochores as expected. Since these SKOV-3 cells are not overexpressing km23-1-Flag, there is no Flag staining. However, in these +Dox cells at metaphase, there is no detectable BubR1 at the kinetochore. We have used two different BubR1 antibodies from two different companies, and both of these reveal no detectable BubR1 staining in the Dox+ metaphase cells. To confirm that a decrease in overall BubR1 expression did not account for the absence of kinetochore BubR1 at metaphase in the +Dox cells, we performed Western blot analysis during the 9-14d experimental period and BubR1 levels were not significantly different between the +/−Dox cells (data not shown). Moreover, clear CREST staining indicated that the kinetochore itself was not aberrant in the Dox+ cells, suggesting that the BubR1-related checkpoint has been inactivated.[35-36] Overall, our results suggest that the prolongation of prometaphase/metaphase induced by overexpression of km23-1 is associated with the sustained presence of BubR1 at the kinetochore, consistent with a prolonged activation of the BubR1-related SAC.

Since a disrupted SAC would not only cause a delay prior to anaphase, but could also lead to the formation of multipolar spindles and multinucleated cells, we investigated the spindle polarities of the HOCCs in +/−Dox. Representative photos of α-tubulin staining of MT spindles are shown in Fig. 4C (red), in relation to chromatin staining (DAPI) and Flag staining in the −Dox cells (green). As indicated in Fig. 4C (bottom), induction of km23-1 expression in the −Dox SKOV-3 cells showed a statistically significant increase in the percentage of multipolar spindles (3-fold compared to +Dox). Similarly, km23-1 over-expressing SKOV-3 cells showed a higher percentage of multinuclear cells (3-fold compared to control, Fig. 4D). Overall, these cellular changes suggest that km23-1 induction affected a mitotic delay associated with multinucleation/multipolarity, phenotypes often observed in mitotic catastrophe.[30-31]

As a result of our findings suggesting mitotic catastrophe, it was of interest to assess whether the cells were undergoing apoptosis. Accordingly, we measured the annexin V-positive cells in a cumulative fashion during the 9-14d +/−Dox, when the Flag-positive cells began displaying a mitotic delay. As shown in Fig. 4E, we observed an increased number of apoptotic cells in Dox−/Flag-positive cells, compared to the Dox+ cells. Overall, these cellular changes suggest that the high levels of km23-1 may be inducing a gradual apoptotic death process occurring after mitotic delay.[30-31]

km23-1 inhibits the *in vivo* tumorigenicity of SKOV-3 cells

Since our results thus far suggested that the prometaphase/metaphase delay from km23-1 overexpression might be associated with cell death as a result of mitotic catastrophe,[31] it was of interest to determine whether overexpression of km23-1 in HOCCs would block tumor formation *in vivo*. *In vivo* tumorigenicity studies[23, 24] were performed as described in "Materials and Methods." Tumor volumes for mice inoculated with EV pool cells and fed with Dox+/− chow were not significantly different throughout the experimental period (Fig. 5A). In contrast, tumors from mice inoculated with km23-1 pool or km23-1 clone #14 cells (−Dox chow) were significantly smaller when compared to controls (+Dox chow, Figs. 5B/

C). Western blot analyses of km23-1 expression in the resected tumor tissues confirmed that km23-1 expression was still induced in the Dox-group at the termination of the experiment (Fig. 5D). Thus, the *in vivo* tumorigenicities of SKOV-3 cells were substantially inhibited by the sustained high levels of km23-1 expression.

Discussion

Our results demonstrate that forced expression of km23-1 causes a growth suppressive phenotype in HOCCs. First, induction of km23-1 expression inhibited both the monolayer and anchorage-independent growth of HOCCs. In addition, FACS analyses in SKOV-3, IGROV-1, and OVCA433 HOCCs demonstrate that there was an increase in the fraction of cells at G2/M. Furthermore, the phospho-histone H3 and $\tilde{\alpha}$tubulin staining data indicate that the overexpression of km23-1 caused a mitotic delay at prometaphase/metaphase. This was associated with high levels of phospho-MEK, phospho-ERK, and cyclin B1, indicating that the cells had not yet progressed to anaphase. Most importantly, km23-1 overexpression reduced the tumorigenic potential of SKOV-3 cells in a xenograft model. Overall, these results demonstrate that km23-1 suppresses HOCC growth by causing a delay in prometaphase/metaphase, and suggest that km23-1 is a critical growth regulator for HOCCs.

km23-1 was originally identified as a TGFß receptor-interacting protein and was shown to be required for TGFß-dependent Smad2 signaling.[6, 10, 12-14] Further, in cells expressing normal levels of km23-1, knockdown of its expression was associated with a decrease in the percentage of cells in G2/M and a blockade of dynein-mediated transport.[10, 12] In contrast, here we reveal a novel role for this DLC in mitosis. This novel role is distinct from km23-1's role in TGFß-mediated growth inhibition that occurs by blocking the cell cycle in late G1 in untransformed epithelial cells.[12] The focus of the current report is on km23-1's ability to alter events in mitosis in TGFß-resistant HOCCs.

Our data demonstrate that km23-1 inhibited HOCC growth by prolonging mitosis with up-regulated cyclin B1 protein expression levels and elevated phospho-MEK and phospho-ERK. Since the destruction of cyclin B1 starts at the end of prometaphase, with most of the cyclin B1 being degraded by the end of metaphase,[32, 33] our data suggest that the mitotic delay occurred prior to anaphase. Further, it has been reported that the poleward transport of MEK1/2 at the SAC in prometaphase/metaphase is dynein-mediated.[34] Thus, the finding that MEK and ERK remain activated in the km23-1 over-expressing cells suggests that the high levels of km23-1 may be disrupting the normal functions of km23-1 in the dynein-mediated streaming of mitotic checkpoint protein complexes away from the kinetochore to inactivate the SAC.

As mentioned above, the high levels of km23-1 appeared to regulate the HOCCs in a manner consistent with an effect in mitosis at the SAC. In km23-1-overexpressing SKOV-3 cells at prometaphase, km23-1 was co-localized with the SAC protein BubR1 at the kinetochore. In contrast, by metaphase, BubR1 was no longer co-localized with km23-1, but it abnormally remained at the kinetochore. This persistent localization of BubR1 at the kinetochore in metaphase suggests that the SAC remains active in km23-1 over-expressing cells. Persistent localization of BubR1 at the kinetochore with an activated SAC has been reported by others as well.[35, 36] In contrast, in the HOCCs not over-expressing km23-1, BubR1 was no longer visible at the kinetochore in metaphase, suggesting that it had been removed by the normal dynein-mediated streaming events that occur during inactivation of the SAC.[4, 5] These cells would then continue on to anaphase. Overall then, our results demonstrate that km23-1 suppresses HOCC growth by causing a delay in metaphase through a BubR1-related mechanism.

In relation to dynein functions at the SAC, to date, most studies have focused on cytoplasmic dynein subunits other than the regulatory/adaptor DLCs (ie, on the dynein heavy chain, dynein light intermediate chain (DLIC), DIC). For example, the DLIC has been shown to remove the Mad1 and Mad2 checkpoint proteins from the kinetochore during SAC silencing, but not BubR1.[37] Perhaps the km23-1 DLC is normally responsible for stripping BubR1 from the kinetochore, but when it is over-expressed, this is aberrant or lost. There is one report describing the involvement of a member of another class of DLCs (DYNLT3) at the SAC through its interaction with the mitotic checkpoint protein Bub3.[38] However, this report did not address a role for DLCs in tumor suppression as we have done herein.

While overexpression of km23-1 may be affecting BubR1 transport away from the kinetochore to inactivate the SAC, there are other possible interpretations for our findings, since dynein is known to have functions in many aspects of spindle MT dynamics.[39-42] For example, the high levels of km23-1 would be expected to alter dynein motor functions in stable MT attachment and maintenance of kinetochore orientation during metaphase chromosome alignment.[39, 43] Thus, an effect of km23-1 on MT-kinetochore interactions and/or dynein availability at the kinetochore would be consistent with a persistent localization of BubR1 at the kinetochore, which would ultimately result in prolonged SAC activation.

The phenotypic changes we have observed upon overexpression of the km23-1 DLC are consistent with the HOCCs undergoing a process referred to as “mitotic catastrophe” or “cell death preceded by multinucleation/multipolarity.”[31, 44] For example, we have shown that overexpression of km23-1 in HOCCs causes altered localization of the SAC protein BubR1 at metaphase, in association with the formation of multipolar, multinucleated, and enlarged cells.[45, 46] In our system, it appears that successive rounds of cell division after mitotic delay eventually lead to cell death, resulting in cell growth inhibition *in vitro* in monolayer culture and in semisolid medium, as well as tumor suppression *in vivo*.

Overall, our results suggest that km23-1 is a novel mitotic tumor inhibitor for ovarian cancer, functioning at metaphase to alter the localization of the SAC protein BubR1, associated with mitotic catastrophe and eventual cell death. Along these lines, it has recently been reported that targeting the SAC and chromosome alignment simultaneously, may selectively kill tumor cells.[47] Thus, km23-1-based therapeutics designed to mimic the effects of over-expressed km23-1 may have potential for the treatment of ovarian cancer. Similar approaches have been employed for the tumor suppressor p53.[48] Alternatively, km23-1-based therapeutics may sensitize tumor cells to clinically relevant doses of taxol, as has been described for other therapeutic approaches.[47] Additionally, a combined approach may be required rather than using a single therapeutic modality. This is often necessary due to the higher complexity of *in vivo* conditions[49, 50] compared to *in vitro* responses, as we have seen here. Future studies will address these potential therapeutic approaches.

Acknowledgments

This work was supported by National Institutes of Health grants CA100239, CA90765, and CA92889, as well as Department of Defense award DAMD 17-03-1-0287, to K.M.M. pBig2r vector was a gift from G. Robertson, Penn State College of Medicine (Hershey, PA). We also thank N. Sheaffer and D. Stanford (Cell Science & Flow Cytometry Core Lab, Penn State Hershey Cancer Institute) for FACS technical support. Core Facility services and instruments used in this project were funded, in part, under a grant with the Pennsylvania Department of Health using Tobacco Settlement Funds. The PA Department of Health specifically disclaims responsibility for any analyses, interpretations or conclusions.

References

1. Society, AC. Cancer Facts and Figures 2010. American Cancer Society; Atlanta, Ga: 2010. Also available online, Last accessed July 28, 2010
2. Wood KW, Lad L, Luo L, Qian X, Knight SD, Nevins N, Brejc K, Sutton D, Gilmartin AG, Chua PR, Desai R, Schauer SP, et al. Antitumor activity of an allosteric inhibitor of centromere-associated protein-E. Proc Natl Acad Sci U S A. 2010; 107:5839–44. [PubMed: 20167803]
3. Wacker SA, Kapoor TM. Targeting a kinetochore-associated motor protein to kill cancer cells. Proc Natl Acad Sci U S A. 2010; 107:5699–700. [PubMed: 20308538]
4. Wojcik E, Basto R, Serr M, Scaerou F, Karess R, Hays T. Kinetochore dynein: its dynamics and role in the transport of the Rough deal checkpoint protein. Nat Cell Biol. 2001; 3:1001–7. [PubMed: 11715021]
5. Vallee RB, Varma D, Dujardin DL. ZW10 function in mitotic checkpoint control, dynein targeting and membrane trafficking: is dynein the unifying theme? Cell Cycle. 2006; 5:2447–51. [PubMed: 17102640]
6. Tang Q, Staub CM, Gao G, Jin Q, Wang Z, Ding W, Aurigemma RE, Mulder KM. A novel transforming growth factor-beta receptor-interacting protein that is also a light chain of the motor protein dynein. Mol Biol Cell. 2002; 13:4484–96. [PubMed: 12475967]
7. Jiang J, Yu L, Huang X, Chen X, Li D, Zhang Y, Tang L, Zhao S. Identification of two novel human dynein light chain genes, DNLC2A and DNLC2B, and their expression changes in hepatocellular carcinoma tissues from 68 Chinese patients. Gene. 2001; 281:103–13. [PubMed: 11750132]
8. Bowman AB, Patel-King RS, Benashski SE, McCaffery JM, Goldstein LS, King SM. Drosophila roadblock and Chlamydomonas LC7: a conserved family of dynein-associated proteins involved in axonal transport, flagellar motility, and mitosis. J Cell Biol. 1999; 146:165–80. [PubMed: 10402468]
9. Pfister KK, Fisher EM, Gibbons IR, Hays TS, Holzbaur EL, McIntosh JR, Porter ME, Schroer TA, Vaughan KT, Witman GB, King SM, Vallee RB. Cytoplasmic dynein nomenclature. J Cell Biol. 2005; 171:411–3. [PubMed: 16260502]
10. Jin Q, Ding W, Mulder KM. Requirement for the dynein light chain km23-1 in a Smad2-dependent transforming growth factor-beta signaling pathway. J Biol Chem. 2007; 282:19122–32. [PubMed: 17420258]
11. Couwenbergs C, Labbe JC, Goulding M, Marty T, Bowerman B, Gotta M. Heterotrimeric G protein signaling functions with dynein to promote spindle positioning in C. elegans. J Cell Biol. 2007; 179:15–22. [PubMed: 17908918]
12. Jin Q, Ding W, Staub CM, Gao G, Tang Q, Mulder KM. Requirement of km23 for TGFbeta-mediated growth inhibition and induction of fibronectin expression. Cell Signal. 2005; 17:1363–72. [PubMed: 15925487]
13. Ilangovan U, Ding W, Zhong Y, Wilson CL, Groppe JC, Trbovich JT, Zuniga J, Demeler B, Tang Q, Gao G, Mulder KM, Hinck AP. Structure and dynamics of the homodimeric dynein light chain km23. J Mol Biol. 2005; 352:338–54. [PubMed: 16083906]
14. Jin, Q.; Gao, G.; Mulder, KM. Involvement of km23 light dynein chains in TGF beta signaling. In: Jakowlew, SB., editor. Transforming Growth Factor-beta in Cancer Therapy. Vol. 1. Humana Press Inc; Totowa, NJ: 2008. p. 169-184.
15. Baldwin RL, Tran H, Karlan BY. Loss of c-myc repression coincides with ovarian cancer resistance to transforming growth factor beta growth arrest independent of transforming growth factor beta/Smad signaling. Cancer Res. 2003; 63:1413–9. [PubMed: 12649207]
16. Hu W, Wu W, Nash MA, Freedman RS, Kavanagh JJ, Verschraegen CF. Anomalies of the TGF-beta postreceptor signaling pathway in ovarian cancer cell lines. Anticancer Res. 2000; 20:729–33. [PubMed: 10810347]
17. Strathdee CA, McLeod MR, Hall JR. Efficient control of tetracycline-responsive gene expression from an autoregulated bi-directional expression vector. Gene. 1999; 229:21–9. [PubMed: 10095100]

18. Jin Q, Gao G, Mulder KM. Requirement of a dynein light chain in TGFbeta/Smad3 signaling. J Cell Physiol. 2009; 221:707–15. [PubMed: 19711352]
19. Mulder KM, Ramey MK, Hoosein NM, Levine AE, Hinshaw XH, Brattain DE, Brattain MG. Characterization of transforming growth factor-beta-resistant subclones isolated from a transforming growth factor-beta-sensitive human colon carcinoma cell line. Cancer Res. 1988; 48:7120–5. [PubMed: 3191488]
20. Howell BJ, McEwen BF, Canman JC, Hoffman DB, Farrar EM, Rieder CL, Salmon ED. Cytoplasmic dynein/dynactin drives kinetochore protein transport to the spindle poles and has a role in mitotic spindle checkpoint inactivation. J Cell Biol. 2001; 155:1159–72. [PubMed: 11756470]
21. Beltrami E, Plescia J, Wilkinson JC, Duckett CS, Altieri DC. Acute ablation of survivin uncovers p53-dependent mitotic checkpoint functions and control of mitochondrial apoptosis. J Biol Chem. 2004; 279:2077–84. [PubMed: 14581472]
22. Ohishi T, Hirota T, Tsuruo T, Seimiya H. TRF1 mediates mitotic abnormalities induced by Aurora-A overexpression. Cancer Res. 2010; 70:2041–52. [PubMed: 20160025]
23. Yu D, Wolf JK, Scanlon M, Price JE, Hung MC. Enhanced c-erbB-2/neu expression in human ovarian cancer cells correlates with more severe malignancy that can be suppressed by E1A. Cancer Res. 1993; 53:891–8. [PubMed: 8094034]
24. Wu SP, Theodorescu D, Kerbel RS, Willson JK, Mulder KM, Humphrey LE, Brattain MG. TGF-beta 1 is an autocrine-negative growth regulator of human colon carcinoma FET cells in vivo as revealed by transfection of an antisense expression vector. J Cell Biol. 1992; 116:187–96. [PubMed: 1730743]
25. Wolf F, Wandke C, Isenberg N, Geley S. Dose-dependent effects of stable cyclin B1 on progression through mitosis in human cells. EMBO J. 2006; 25:2802–13. [PubMed: 16724106]
26. Borysov SI, Cheng AW, Guadagno TM. B-Raf is critical for MAPK activation during mitosis and is regulated in an M phase-dependent manner in Xenopus egg extracts. J Biol Chem. 2006; 281:22586–96. [PubMed: 16762920]
27. Harding A, Giles N, Burgess A, Hancock JF, Gabrielli BG. Mechanism of mitosis-specific activation of MEK1. J Biol Chem. 2003; 278:16747–54. [PubMed: 12609978]
28. Kang J, Yu H. Kinase signaling in the spindle checkpoint. J Biol Chem. 2009; 284:15359–63. [PubMed: 19228686]
29. Logarinho E, Bousbaa H. Kinetochore-microtubule interactions “in check” by Bub1, Bub3 and BubR1: The dual task of attaching and signalling. Cell Cycle. 2008; 7:1763–8. [PubMed: 18594200]
30. Vakifahmetoglu H, Olsson M, Zhivotovsky B. Death through a tragedy: mitotic catastrophe. Cell Death Differ. 2008; 15:1153–62. [PubMed: 18404154]
31. Kroemer G, Galluzzi L, Vandenabeele P, Abrams J, Alnemri ES, Baehrecke EH, Blagosklonny MV, El-Deiry WS, Golstein P, Green DR, Hengartner M, Knight RA, et al. Classification of cell death: recommendations of the Nomenclature Committee on Cell Death 2009. Cell Death Differ. 2009; 16:3–11. [PubMed: 18846107]
32. D’Angiolella V, Grieco D. Attach first, then detach: a role for cyclin B-dependent kinase 1 in coordinating proteolysis with spindle assembly. Cell Cycle. 2004; 3:132–3. [PubMed: 14712073]
33. Clute P, Pines J. Temporal and spatial control of cyclin B1 destruction in metaphase. Nat Cell Biol. 1999; 1:82–7. [PubMed: 10559878]
34. Xiong B, Yu LZ, Wang Q, Ai JS, Yin S, Liu JH, OuYang YC, Hou Y, Chen DY, Zou H, Sun QY. Regulation of intracellular MEK1/2 translocation in mouse oocytes: cytoplasmic dynein/dynactin-mediated poleward transport and cyclin B degradation-dependent release from spindle poles. Cell Cycle. 2007; 6:1521–7. [PubMed: 17507801]
35. Nitta M, Kobayashi O, Honda S, Hirota T, Kuninaka S, Marumoto T, Ushio Y, Saya H. Spindle checkpoint function is required for mitotic catastrophe induced by DNA-damaging agents. Oncogene. 2004; 23:6548–58. [PubMed: 15221012]
36. Jeffery JM, Urquhart AJ, Subramaniam VN, Parton RG, Khanna KK. Centrobin regulates the assembly of functional mitotic spindles. Oncogene. 2010; 29:2649–58. [PubMed: 20190801]

37. Sivaram MV, Wadzinski TL, Redick SD, Manna T, Doxsey SJ. Dynein light intermediate chain 1 is required for progress through the spindle assembly checkpoint. EMBO J. 2009; 28:902–14. [PubMed: 19229290]
38. Lo KW, Kogoy JM, Pfister KK. The DYNLT3 light chain directly links cytoplasmic dynein to a spindle checkpoint protein, Bub3. J Biol Chem. 2007; 282:11205–12. [PubMed: 17289665]
39. Woodard GE, Huang NN, Cho H, Miki T, Tall GG, Kehrl JH. Ric-8A and Gi alpha recruit LGN, NuMA, and dynein to the cell cortex to help orient the mitotic spindle. Mol Cell Biol. 2010; 30:3519–30. [PubMed: 20479129]
40. Griffis ER, Stuurman N, Vale RD. Spindly, a novel protein essential for silencing the spindle assembly checkpoint, recruits dynein to the kinetochore. J Cell Biol. 2007; 177:1005–15. [PubMed: 17576797]
41. Kardon JR, Vale RD. Regulators of the cytoplasmic dynein motor. Nat Rev Mol Cell Biol. 2009; 10:854–65. [PubMed: 19935668]
42. Gaetz J, Kapoor TM. Dynein/dynactin regulate metaphase spindle length by targeting depolymerizing activities to spindle poles. J Cell Biol. 2004; 166:465–71. [PubMed: 15314063]
43. Varma D, Monzo P, Stehman SA, Vallee RB. Direct role of dynein motor in stable kinetochore-microtubule attachment, orientation, and alignment. J Cell Biol. 2008; 182:1045–54. [PubMed: 18809721]
44. Stevens JB, Liu G, Bremer SW, Ye KJ, Xu W, Xu J, Sun Y, Wu GS, Savasan S, Krawetz SA, Ye CJ, Heng HH. Mitotic cell death by chromosome fragmentation. Cancer Res. 2007; 67:7686–94. [PubMed: 17699772]
45. Li S, Szymborski A, Miron MJ, Marcellus R, Binda O, Lavoie JN, Branton PE. The adenovirus E4orf4 protein induces growth arrest and mitotic catastrophe in H1299 human lung carcinoma cells. Oncogene. 2009; 28:390–400. [PubMed: 18955965]
46. Kwong J, Kulbe H, Wong D, Chakravarty P, Balkwill F. An antagonist of the chemokine receptor CXCR4 induces mitotic catastrophe in ovarian cancer cells. Mol Cancer Ther. 2009; 8:1893–905. [PubMed: 19567818]
47. Janssen A, Kops GJ, Medema RH. Elevating the frequency of chromosome mis-segregation as a strategy to kill tumor cells. Proc Natl Acad Sci U S A. 2009; 106:19108–13. [PubMed: 19855003]
48. Vogelstein B, Kinzler KW. Achilles' heel of cancer? Nature. 2001; 412:865–6. [PubMed: 11528457]
49. Buck E, Eyzaguirre A, Brown E, Petti F, McCormack S, Haley JD, Iwata KK, Gibson NW, Griffin G. Rapamycin synergizes with the epidermal growth factor receptor inhibitor erlotinib in non-small-cell lung, pancreatic, colon, and breast tumors. Mol Cancer Ther. 2006; 5:2676–84. [PubMed: 17121914]
50. Debnath J, Brugge JS. Modelling glandular epithelial cancers in three-dimensional cultures. Nat Rev Cancer. 2005; 5:675–88. [PubMed: 16148884]

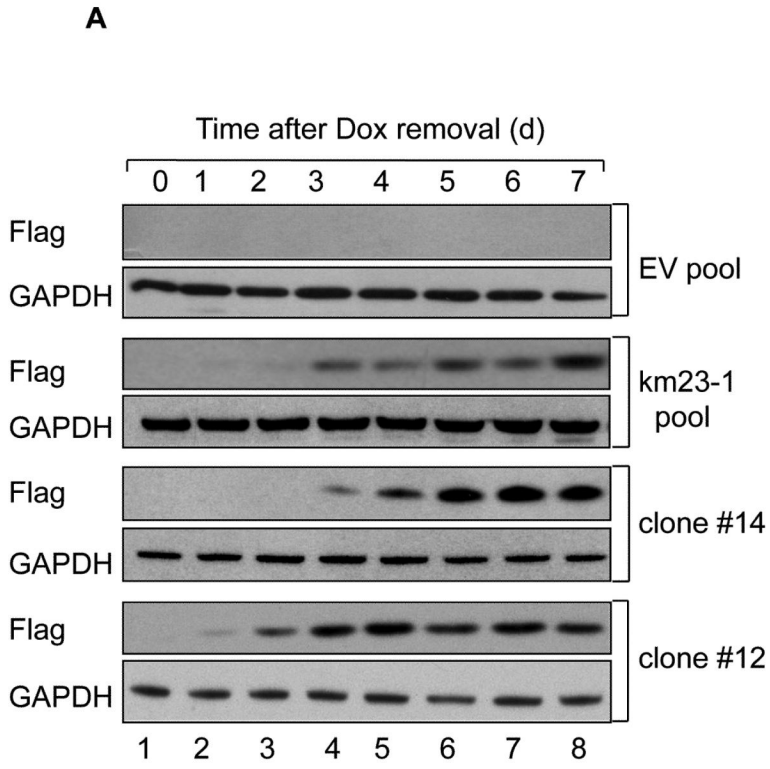

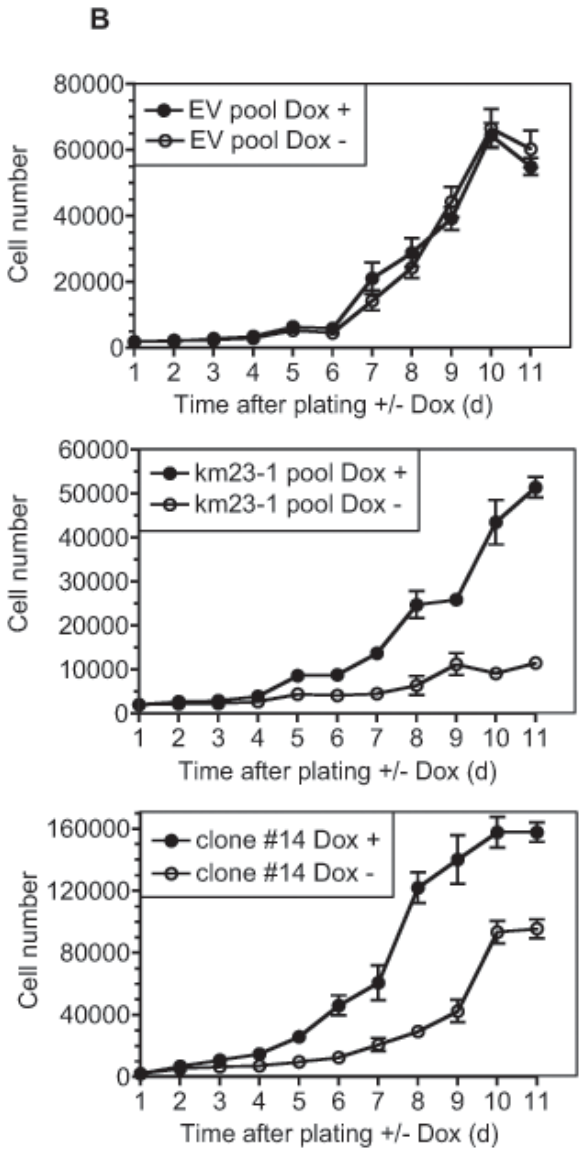

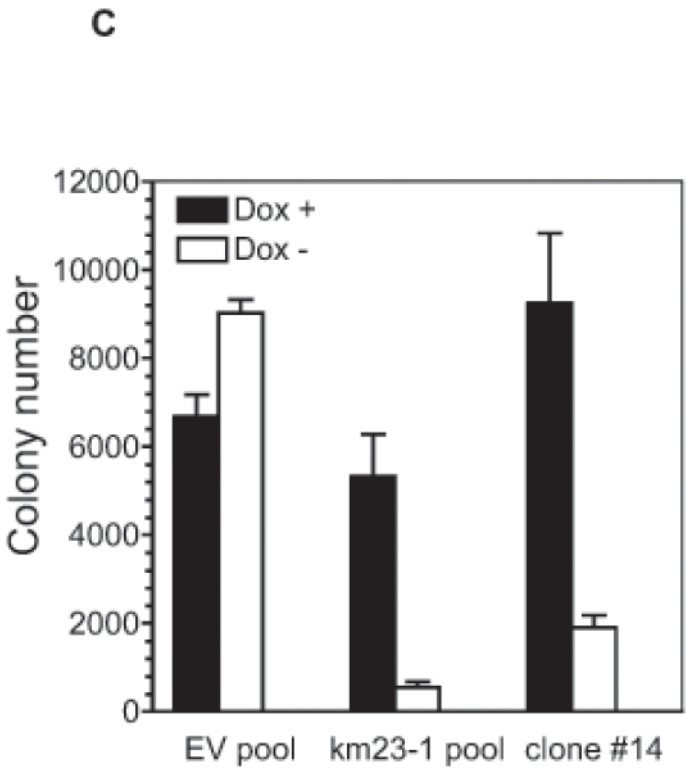

Fig. 1. Overexpression of km23-1 in SKOV-3 cells inhibits monolayer cell proliferation and soft agar colony formation

A. Western blotting was performed following Dox removal for the indicated number of days. **B.** Cells were monitored by crystal violet assay (mean ± SD, n=3 wells), representative of three (EV pool and clone #14) or two (km 23-1 pool) independent experiments. **C.** Soft agar assays were performed as described in "Material and Methods," representative of two independent experiments (mean ± SD, n=3 wells per cell type).

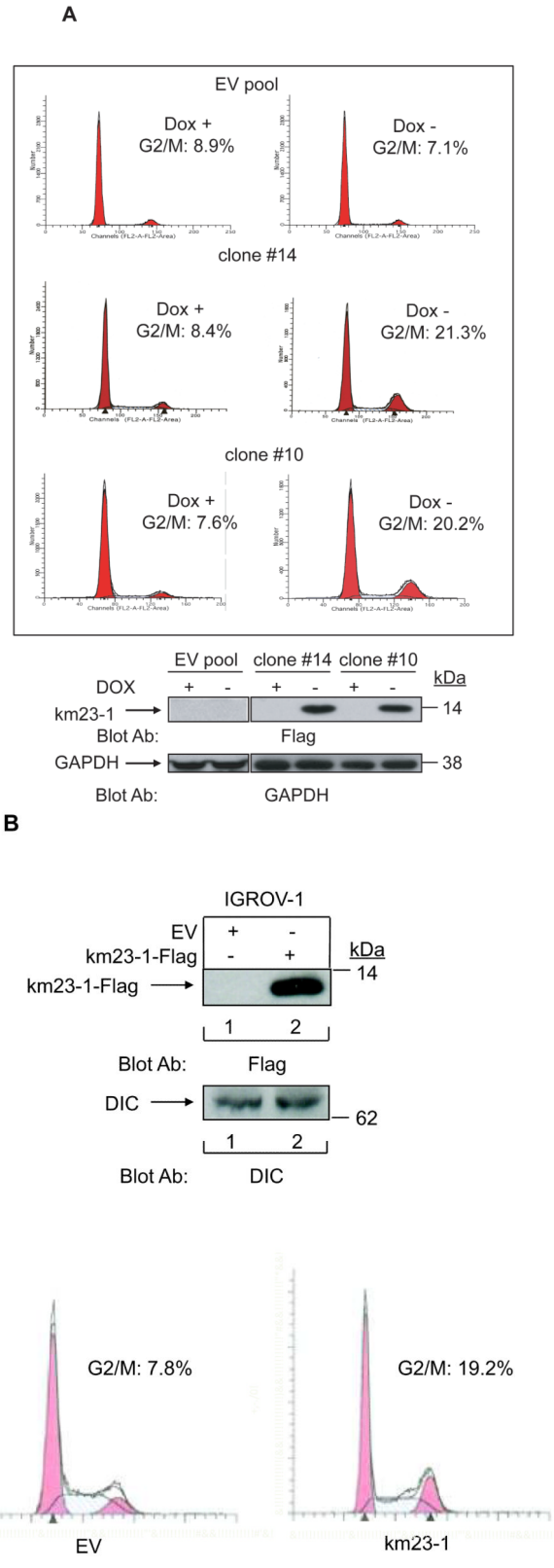

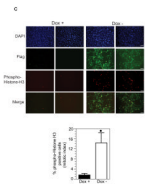

Fig. 2. Overexpression of km23-1 in HOCCs causes a mitotic delay

A, Upper panel, cells were grown in +/−Dox for 9-14d, and cell cycle distribution was determined by FACS analysis. **Lower panel,** Western blotting analysis of Flag expression. The same membrane was reblotted with an anti-GAPDH antibody. **B.** Total cell lysates, collected from IGROV-1 cells that had been transfected with km23-1-Flag or EV for 72h, were analyzed by Western blot analyses using an anti-Flag antibody. The same membrane was reblotted with an anti-DIC antibody to assess equal loading (**top panel**). The transfected cells were also fixed and subjected to FACS analysis (**bottom panel**). **C. Upper panels,** km23-1 clone #14 cells were fixed, permeabilized, and stained as described in "Materials and Methods." Bar=100 μm. **Lower panel**, the percentages of mitotic cells were quantitated as the number of phospho-histone H3-positive cells per the number of Flag expressing cells in mitosis. The bars represent the mean ± SE, n=3; *p<0.05 relative to +Dox controls.

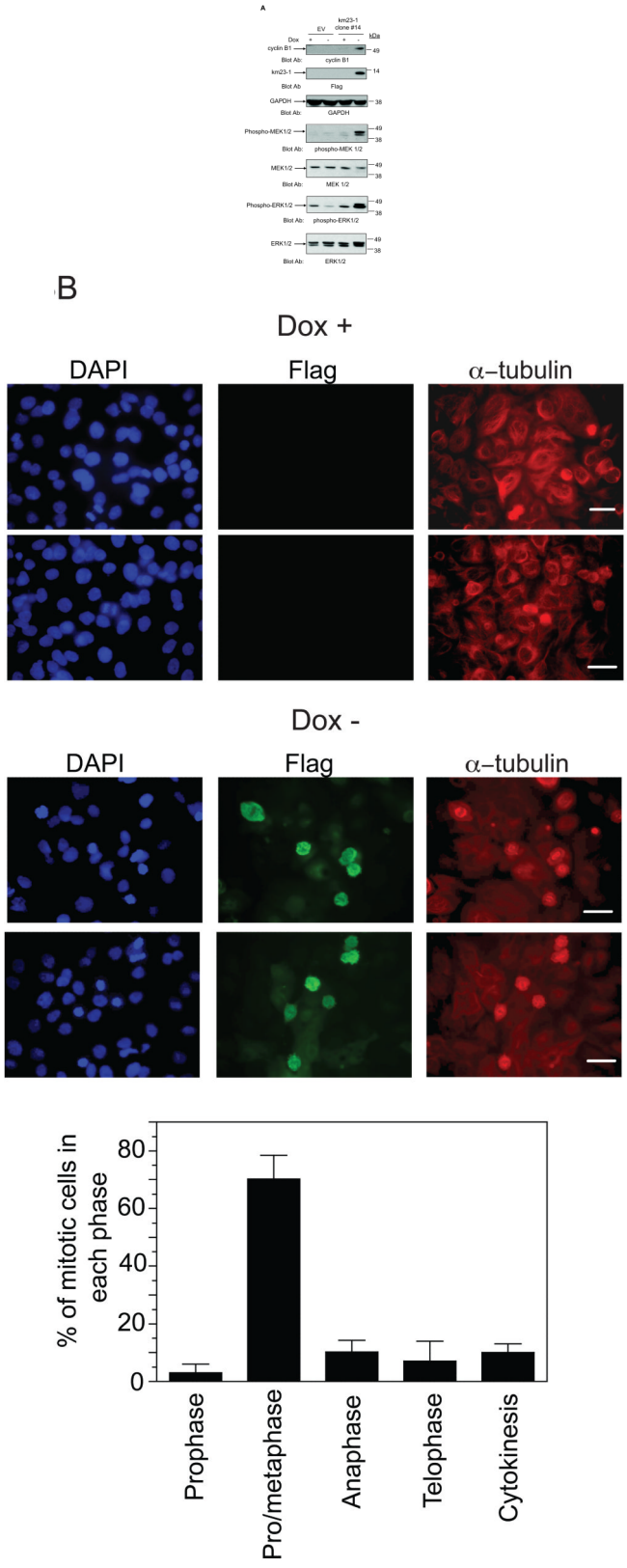

Fig. 3. Induction of km23-1 expression in SKOV-3 cells results in accumulation of cells prior to anaphase at prometaphase/metaphase

A. Western blot analysis was performed using the indicated antibodies. All data are representative of at least two independent experiments. **B. Upper panels,** cells were grown and treated as for Fig. 2, and were stained for DAPI, Flag, and α-tubulin. Bar=25μm. **Lower panel,** mitotic cells were counted using Flag and α-tubulin staining.

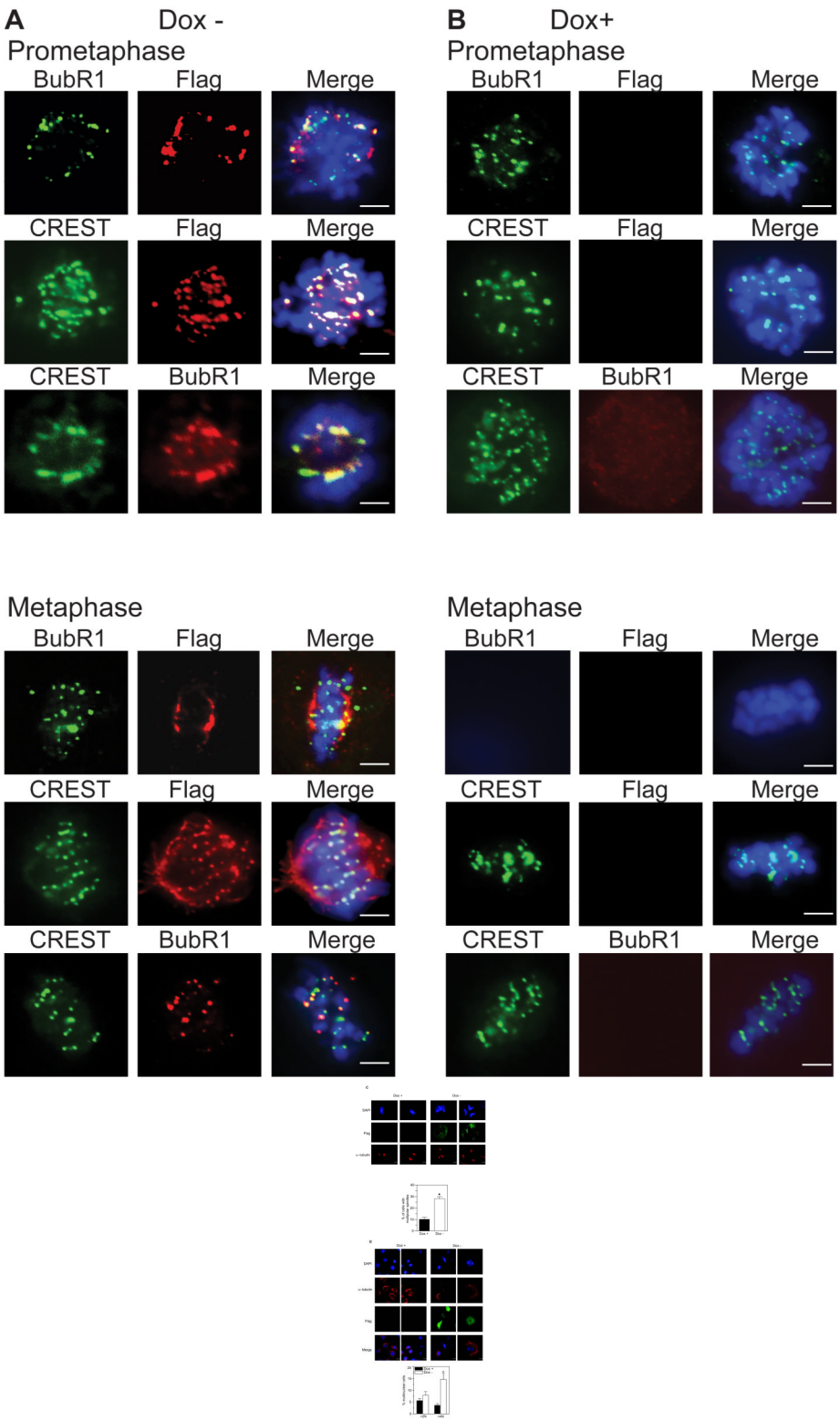

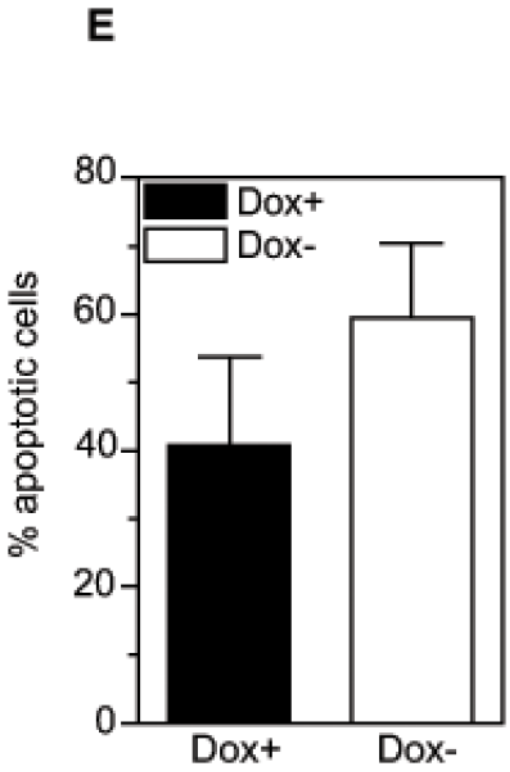

Fig. 4. Overexpression of km23-1 in SKOV-3 cells alters events at the SAC

A. Dox− SKOV-3 cells. km23-1 is present with BubR1 at the kinetochore in **Prometaphase**, whereas **in Metaphase** km23-1 is localized at the kinetochore and/or along MT spindles, while BubR1's localization is aberrant. Kinetochore immunostaining studies in SKOV-3 clone #14 Dox− cells were described in "Materials and Methods". DAPI (blue) staining shows chromosomes. Merge depicts colocalization of the relevant components. **B. Dox+ SKOV-3 cells.** BubR1 is present at the kinetochore of **Prometaphase** SKOV-3 cells, but is absent from the kinetochore by **Metaphase**. Studies were the same as for A, except that normal mitotic Dox+ cells are shown. IgG staining was used as a negative control. Images (1000X) were acquired as described in "Materials and Methods." Bar=10 μm. All data are representative of at least two independent experiments. C. Effects of km23-1 overexpression on spindle polarity. **Upper panels**, studies were performed as for Fig. 3B. Representative images of MT spindles in +/−Dox cells are shown. Bar=5 μm. **Lower panel**, Quantification of multipolar spindles was described in "Materials and Methods." Cells showing multipolar spindles were quantified in +/−Dox cells and compared to either total cell number or to km23-1-Flag-positive cells (mean ± SE, n=3); asterisk, $p<0.05$ relative to +Dox. D. Overexpression of km23-1 increases the percentage of multinuclear cells. Upper panels, images of representative cells. Bar = 10 μm. **Bottom panel,** quantification of multinucleated cells was described in "Materials and Methods" (mean ± SE, n=4; asterisk, $p<0.05$ relative to +Dox; >2N, more than two nuclei; >4N, more than four nuclei). E. Overexpression of km23-1 increases the percentage of apoptotic cells. Data shown were collected in a cumulative fashion during the period when Flag positive cells were undergoing the mitotic delay (mean ± SE, n=3).

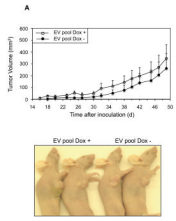

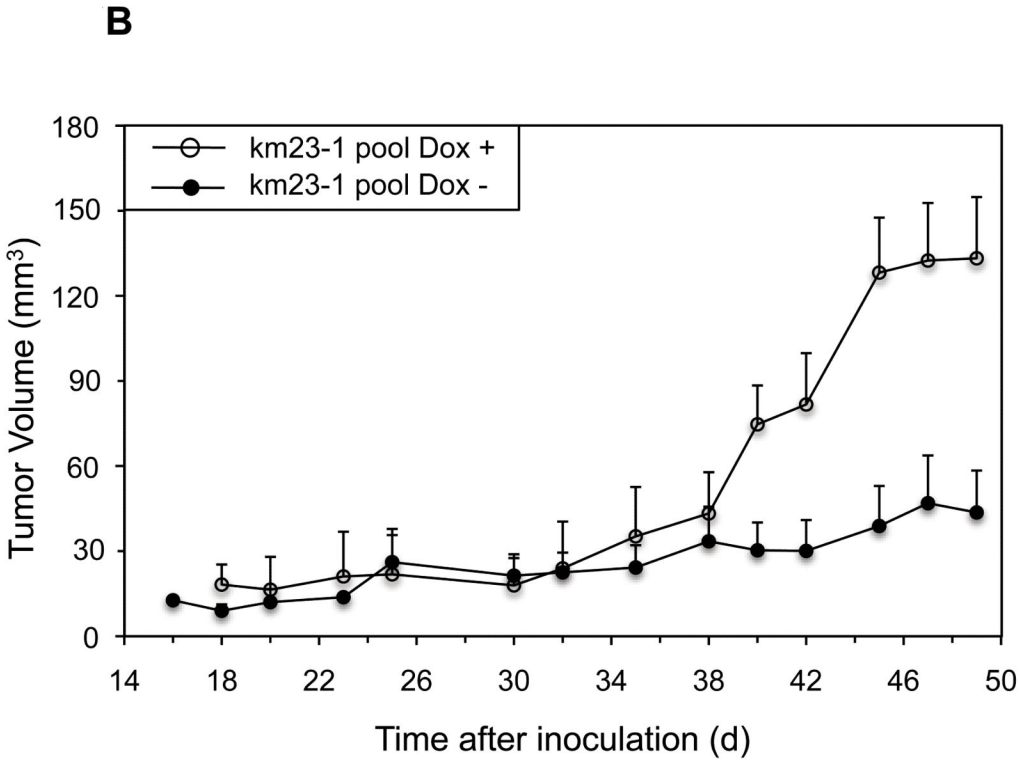

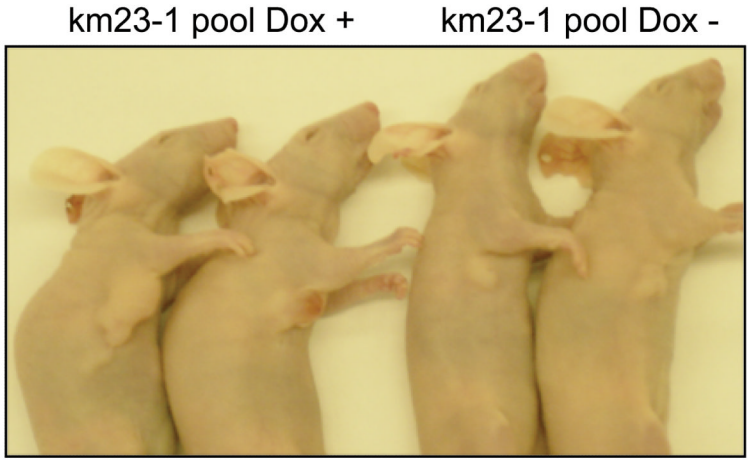

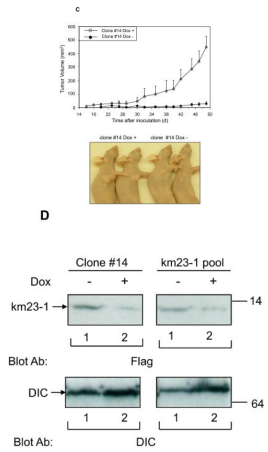

Fig. 5. Induction of km23-1 expression inhibits xenograft tumor growth of SKOV-3 cells *in vivo*

Balb/c nude mice were inoculated subcutaneously as described in "Materials and Methods." Tumor size was assessed at the indicated times by measuring the length and width of the tumor. Tumor volumes were calculated using the formula length X width^2/2 from each of **A.** EV pool; **B.** km23-1 pool; and **C.** clone #14 (mean ± SD, n=8). Photos of two representative mice from each treatment group are shown to indicate the sizes of the resulting tumors. **D.** km23-1-Flag induction is maintained throughout the experimental period in xenograft tumor tissues of −Dox SKOV-3 cells, as measured by Western blot analysis.